Asian Journal of Andrology (2017) 19, 425–432
www.asiaandro.com; www.ajandrology.com

Open Access

ORIGINAL ARTICLE

Erectile Dysfunction

Superparamagnetic iron oxide nanoparticle targeting of adipose tissue-derived stem cells in diabetes-associated erectile dysfunction

Lei-Lei Zhu, Zheng Zhang, He-Song Jiang, Hai Chen, Yun Chen, Yu-Tian Dai

Erectile dysfunction (ED) is a major complication of diabetes, and many diabetic men with ED are refractory to common ED therapies. Adipose tissue-derived stem cells (ADSCs) have been shown to improve erectile function in diabetic animal models. However, inadequate cell homing to damaged sites has limited their efficacy. Therefore, we explored the effect of ADSCs labeled with superparamagnetic iron oxide nanoparticles (SPIONs) on improving the erectile function of streptozotocin-induced diabetic rats with an external magnetic field. We found that SPIONs effectively incorporated into ADSCs and did not exert any negative effects on stem cell properties. Magnetic targeting of ADSCs contributed to long-term cell retention in the corpus cavernosum and improved the erectile function of diabetic rats compared with ADSC injection alone. In addition, the paracrine effect of ADSCs appeared to play the major role in functional and structural recovery. Accordingly, magnetic field-guided ADSC therapy is an effective approach for diabetes-associated ED therapy.

Asian Journal of Andrology (2017) **19**, 425–432; doi: 10.4103/1008-682X.179532; published online: 6 May 2016

Keywords: erectile dysfunction; magnetic targeting; stem cells; superparamagnetic iron oxide nanoparticles

INTRODUCTION

Erectile dysfunction (ED) is a common complication of diabetes in men. The incidence of ED in diabetic men is up to 75%, which is 3 times higher than that in nondiabetic men.[1,2] Diabetic ED (DED) is multifactorial, including etiology, advancing age, duration of diabetes, poor glycemic control, hypertension, hyperlipidemia, sedentary lifestyle, smoking, and the presence of other diabetic complications, which have been shown to be associated with DED in a cross-sectional study.[1] Therefore, the proposed mechanisms of DED are related to vasculopathy, neuropathy, visceral adiposity, insulin resistance, and hypogonadism.[2] A more in-depth discussion of the pathophysiology is available in reviews elsewhere.[3,4] The efficacy of oral medications such as tadalafil, vardenafil, and sildenafil, which are generally considered as first-line treatments for ED, is lower in these patients compared with nondiabetic patients.[5] Recent studies have focused on cellular therapy of DED, and each cell type has been shown to be effective in an animal study.[6] Stem cells restore impaired endothelial cell and cavernous smooth muscle cell functions in DED by secreting multiple growth factors, preventing programmed endothelial cell death, and differentiating into smooth muscle and endothelial cells.[7–11]

Intracavernous (IC) injection of cultured adipose tissue-derived stem cells (ADSCs) has improved erectile function and increased the contents of smooth muscle and endothelial cells in a rat model of DED.[12] However, the main route of stem cell delivery, i.e., IC injection, transfers cells directly into the target site, and thus very few labeled ADSCs are found in the corpus cavernosum, which limits the therapeutic potential.[13] Hence, promoting ADSC engraftment at the target site is of critical importance.

Superparamagnetic iron oxide nanoparticles (SPIONs) are conventional magnetic resonance imaging contrast agents that have been studied extensively for stem cell labeling in recent years.[14,15] These studies have demonstrated that SPIONs can be incorporated into cells *in vitro* and then guided to target areas using an external magnetic field.[16,17] However, even though most studies have shown that SPION labeling does not alter the viability, proliferation or functional properties of stem cells, the effect of SPION labeling on stem cells is still controversial.[18–20] Further, *in vivo* investigations are needed to elucidate the influence of SPION labeling on the therapeutic efficacy of mesenchymal stem cells (MSCs). Indeed, the inconsistencies among studies may be related to the stem cell source, particle size, surface-coating material, incubation time, transfection agent, or labeling technique.[21]

In this study, we first explore the effect of ADSCs labeled with SPIONs on improving the erectile function of streptozotocin (STZ)-induced diabetic rats using an external magnetic field. We hypothesized that (1) ADSCs maintain their biological characteristics after labeling with an appropriate concentration of SPIONs, (2) such labeled cells can be guided to the target site by external magnetic fields, and (3) the therapeutic efficacy is positively correlated with the retention rate of ADSCs at the target site.

MATERIALS AND METHODS

Animals

A total of 42 male, 10-week-old Sprague-Dawley rats were obtained from the Animal Breeding Center at the Affiliated Drum Tower

Department of Andrology, Drum Tower Hospital, School of Medicine, Nanjing University, Nanjing 210008, China.
Correspondence: Dr. YT Dai (13913957628@163.com)
Received: 23 September 2015; Revised: 17 November 2015; Accepted: 23 February 2016

Hospital, School of Medicine, Nanjing University, Nanjing, China. The experiments were approved by the Institutional Animal Care and Use Subcommittee of our university. Eight Sprague-Dawley rats were randomly selected as nondiabetic controls (Control, $n = 8$). The other 34 rats were intraperitoneally injected with STZ to induce type-1 diabetes according to our previously published protocol.[22] Rats with serum glucose levels of >300 mg dl^{-1} (16.6 mmol l^{-1}) were included in the study (28 rats in total). These rats were treated with phosphate-buffered saline (PBS) (DED, $n = 8$), ADSCs labeled with SPIONs (ADSCs, $n = 10$), and SPION-labeled ADSCs with magnetic field application (M-ADSCs, $n = 10$). Blood glucose levels and body weights were monitored regularly during the study. At 4 weeks after treatment, all rats underwent erectile function evaluation. The animals were then sacrificed and the penis was harvested for histology.

ADSC isolation, identification, and 5-ethynyl-2'-deoxyuridine (EdU) labeling

ADSCs were isolated from paratesticular fat of all animals and cultured as described previously.[23] Surface markers were identified by flow cytometric analysis of passage 3 ADSCs. Briefly, 1×10^5 ADSCs were harvested and suspended in 500 μl PBS and incubated with phycoerythrin (PE)-conjugated anti-CD90 (BD Bioscience, Sparks, MD, USA), fluorescein isothiocyanate-conjugated anti-CD34 (Santa Cruz Biotechnology, Santa Cruz, CA, USA), PE-conjugated anti-CD45 (BD Bioscience), or PE-conjugated anti-CD44 (BD Bioscience) antibodies for 15 min at room temperature while protected from light. After washing with PBS 3 times, ADSCs were analyzed using an FACSCalibur (BD Bioscience). Data were analyzed with CellQuest software (BD Biosciences). ADSCs incubated with isotype-matched fluorescent dye-conjugated IgG were used as negative controls.

For cell tracking, ADSCs were labeled with 10 μmol l^{-1} EdU (Invitrogen, Carlsbad, CA, USA) according to the manufacturer's instructions.

Prussian blue staining

Loading of SPIONs into ADSCs and the labeling efficiency were confirmed by Prussian blue staining. Briefly, passage three ADSCs were seeded in 6-well plates and cultured with ADSC medium containing SPIONs (Sigma-Aldrich, St. Louis, MO, USA) at various concentrations (0, 1, 10, 20, 50, and 100 μg Fe ml^{-1}) for 24 h. After incubation, the medium was removed, and the cells were washed 3 times with PBS. Following fixation for 10 min in 4% paraformaldehyde at room temperature, the cells were incubated in a Prussian blue staining solution (1:1 mixture of 1 mol l^{-1} hydrochloric acid and potassium ferrocyanide [Sigma-Aldrich, St. Louis, MO, USA]) for 30 min.

Viability and proliferation of SPION-ADSCs

In vitro toxicity experiments were performed at 24 h after SPION labeling. The methods used to assess cell viability and proliferation were trypan blue exclusion (Sigma-Aldrich, St. Louis, MO, USA) and an MTT assay (KeyGEN BioTECH, Nanjing, China) following the manufacturers' instructions. SPIONs that exhibited the least cytotoxicity were used for the rest of the *in vitro* and *in vivo* experiments.

Intracellular iron determination

To quantify intracellular iron after SPION labeling, the cells (1×10^6) were lysed in 0.4% sodium hydroxide and then a 36% hydrochloric acid aqueous solution. The intracellular iron content was measured with an Atomic Absorption Spectrophotometer (AFS-820, Beijing, China) and expressed as pg of iron per cell.

In vitro and in vivo cell capture experiments

For the *in vitro* magnetic field attraction test, SPION-labeled ADSCs (2×10^5) were resuspended in culture medium and plated onto a 10-cm dish. A 1.3-T magnet was placed directly under the dish for 24 h according to Li *et al*.[24] After 24 h, cell condensation by magnetic capturing was visually examined by Prussian blue staining.

For *in vivo* experiments, IC transplantation of ADSCs was performed as described previously.[7,25] All animals were anesthetized with isoflurane, and a 1.5-cm oblique incision was made to expose the penis. The corpus cavernosum was then gently cannulated using a 28-gauge needle, and each rat received an injection of either 0.5 ml PBS (Cont. and DED groups) or 1×10^6 ADSCs in 0.5 ml PBS (ADSC and M-ADSC groups) into the left corpus cavernosum. In M-ADSC group, the 1.3-T magnet was placed under the injection site for 30 min. Following the injection, the incision was closed in one layer with an absorbable suture.

Determination of erectile function

The intracavernous pressure (ICP) response to electric stimulation of the cavernous nerve was measured as described previously.[10] Briefly, the mean arterial pressure (MAP) and ICP were recorded by an RM6042B/C multichannel signal collection processing system (Chengdu Implement Company, Chengdu, China). The peak ICP/MAP ratio was calculated to evaluate erectile function.

Immunofluorescence

For immunofluorescence staining, tissues and sections were prepared as described previously by us.[10] Briefly, penile sections were incubated with mouse anti-alpha smooth muscle actin (α-SMA, 1:400; Abcam Inc., Cambridge, MA, USA) or anti-von Willebrand factor (vWF, 1:400; Abcam Inc., Cambridge, MA, USA) antibodies at 4°C overnight, followed by fluorescein isothiocyanate-conjugated goat anti-rabbit IgG (Google Organisms, Wuhan, China, 1:500) for 1 h at room temperature. Then, the tissue sections were stained with Click-iT™ reaction cocktail (Invitrogen) and 4,6-diamidino-2-phenylindole (DAPI; Invitrogen). Fluorescence images were captured using a laser scanning confocal fluorescence microscope (Olympus, Williston, VT, USA).

Immunohistochemical staining

All immunohistochemical staining procedures were performed according to a previously described protocol.[10] Briefly, representative sections were incubated with 3% bovine serum albumin for 30 min at room temperature and then rabbit anti-α-SMA (1:200; Abcam Inc., Cambridge, MA, USA), rabbit anti-von Willebrand factor (vWF, 1:200; Abcam Inc., Cambridge, MA, USA), or rabbit anti-vascular endothelial growth factor (VEGF, 1:200; Santa Cruz Biotechnology) antibodies at 4°C overnight, followed by a biotinylated-conjugated secondary antibody (1:200; Boster, Wuhan, Hubei, China). Nuclei were stained with DAPI. α-SMA-, vWF-, and VEGF-stained areas within the corpus cavernosum were analyzed by Image-Pro Plus 6.0 (Media Cybernetics, Silver Spring, MD, USA). Six sections of each penile sample were analyzed, and the average results were calculated for data analysis.

Statistical analysis

All data were presented as the mean ± standard deviation. Statistical analysis was carried out by the independent Student's *t*-test and one-way analysis of variance followed by the Tukey–ramer test for *post hoc* comparisons using SPSS 16.0 software (SPSS Inc., Chicago, IL, USA). $P < 0.05$ was considered statistically significant.

RESULTS

General data of diabetic rats

The body weight and blood glucose levels of rats are shown in **Table 1**. Among 34 rats injected with STZ, 28 rats with blood glucose higher than 300 mg dl^{-1} were chosen as diabetic rats. After 8 weeks, the body weights were significantly lower ($P < 0.01$) and blood glucose levels were significantly higher ($P < 0.01$) in diabetic rats than in control rats. After treatment, body weight and blood glucose levels did not change significantly.

Characterization of ADSCs

Rat ADSCs were isolated from paratesticular fat. After 6 days in culture, ADSCs exhibited a fibroblastic morphology *in vitro* (**Figure 1a**). Flow cytometric analysis showed that most ADSCs expressed typical MSC markers, including CD90 (100.0%) and CD44 (98.9%), and had low expression of hematopoietic markers CD45 (2.13%) and CD34 (0.05%) (**Figure 1b–1e**). These results indicated that the cultured cells were highly pure ADSCs.

Table 1: Body weight and blood glucose (mean±s.d.)

	Control	*DM*	*ADSCs*	*M-ADSCs*
Initial				
BW (g)	221.52±17.1	218.34±18.5	221.37±14.2	205.86±16.3
BG (mg dl^{-1})	118.6±13.8	112.5±11.2	110.2±12.1	116.5±11.8
8 weeks				
BW (g)	435.76±42.9	265.31±26.3*	273.24±33.4*	281.57±42.6*
BG (mg dl^{-1})	108.16±11.3	453.6±57.6*	445.3±65.2*	438.5±59.7*
12 weeks				
BW (g)	483.63±44.6	236.51±32.3*	228.33±44.3*	247.65±39.7*
BG (mg dl^{-1})	116.2±12.8	465.5±53.1*	484.2±42.6*	447.1±39.6*

*P<0.01 compared with control. BW: body weight; BG: blood glucose; s.d.: standard deviation; DM: diabetes mellitus; ADSCs: adipose tissue-derived stem cells; M-ADSCs: ADSCs with magnetic field application

Cellular internalization of SPIONs

The labeling efficiency and cellular uptake were analyzed by Prussian blue staining. No morphological differences were found between labeled and unlabeled cells (**Figure 2a–2f**). The labeled cells displayed the typical blue color whereas unlabeled cells did not exhibit blue staining. When incubated with SPIONs (50 μg ml^{-1}), almost every ADSC showed blue-stained deposits (**Figure 2e**). The cell proliferation assay revealed that SPION labeling (50 μg ml^{-1}) did not affect the proliferation of ADSCs compared with that of unlabeled cells (**Figure 2g**, $P > 0.05$). However, when ADSCs were incubated with a higher concentration (100 μg ml^{-1}) of SPIONs, the optical density value could not be measured accurately because of excessive iron deposition. Trypan blue staining showed that the survival rate of ADSCs was 88.7 ± 6.8% when incubated with 50 μg ml^{-1} SPIONs (**Figure 2h**). Quantification of intracellular iron by atomic absorption spectroscopic measurement (**Figure 2i**) revealed a positive correlation between intracellular iron and the concentration of SPIONs. Thus, ADSCs labeled with SPIONs at a concentration of 50 μg ml^{-1} were used for the following experiments.

Magnetic field attraction in vitro and in vivo

When a magnetic field (1.3 T) was applied to the bottom of the cell culture dish, a clear accumulation of SPION-labeled ADSCs was observed at the edge of the magnet, suggesting that the external magnetic field attracted SPION-labeled ADSCs (**Figure 3a** and **3b**). For the *in vivo* experiments, a magnet (1.3 T) was placed under the

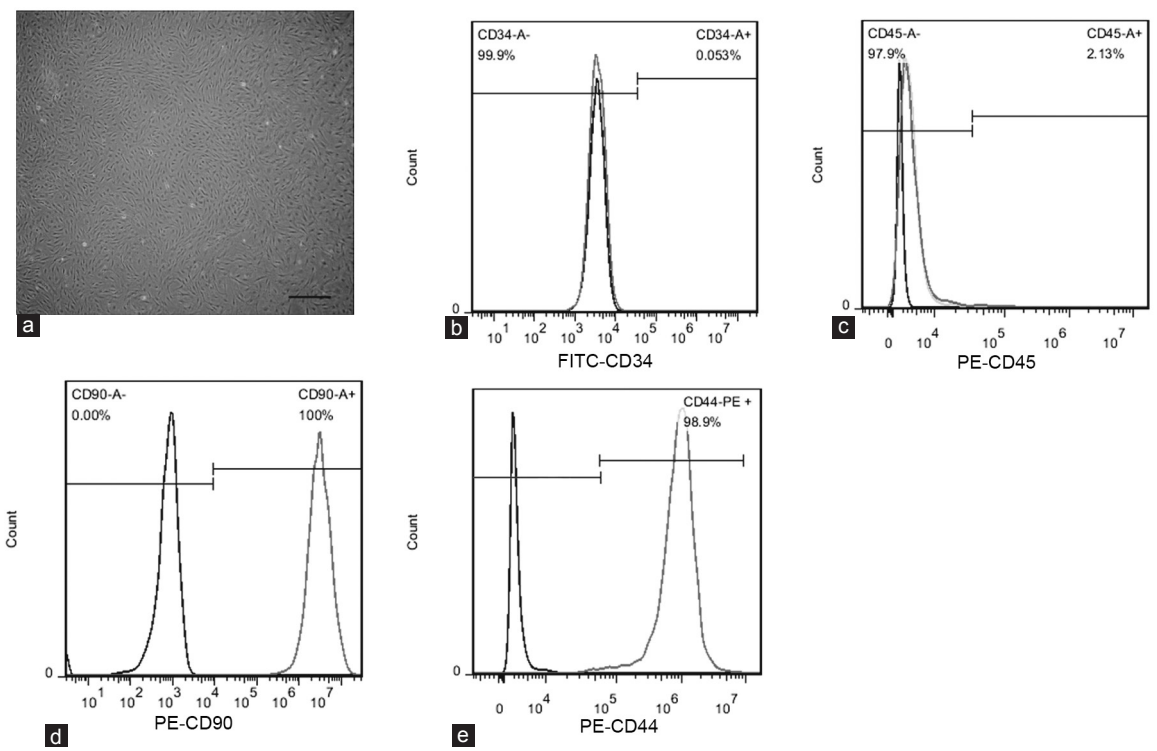

Figure 1: Characterization of rat ADSCs. (**a**) Phase-contrast images showing the fibroblastic morphology of ADSCs. Scale bar = 100 μm. (**b–e**) Flow cytometric analysis showing that cultured ADSCs expressed CD90 and CD44, but not CD34 or CD45. Black curve indicates ADSCs stained with isotype-matched fluorescent dye-conjugated IgG as the negative control; gray curve indicates ADSCs stained with fluorescent dye-conjugated primary antibodies. ADSC: adipose tissue-derived stem cell.

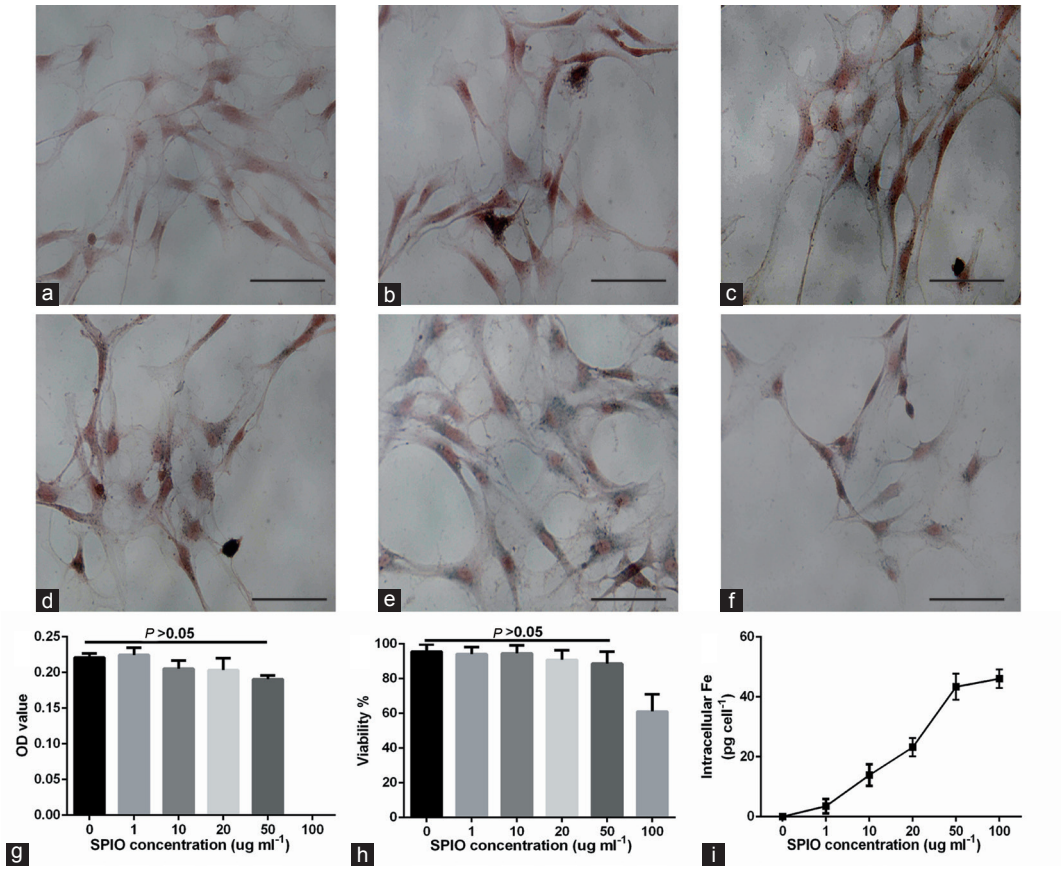

Figure 2: Cellular internalization of SPIONs. (**a–f**) Photomicrographs showing the morphology of ADSCs incubated with SPIONs at concentrations of 0, 1, 10, 20, 50, and 100 μg ml^{-1}. Scale bars = 20 μm. (**g** and **h**) Bar graph showing quantification of cell proliferation and viability at the above SPION concentrations by an MTT assay and trypan blue staining, respectively. (**i**) Bar graph showing quantification of iron uptake by cells at each of the abovementioned SPION concentrations by atomic absorption spectroscopic measurement. SPION: superparamagnetic iron oxide nanoparticle.

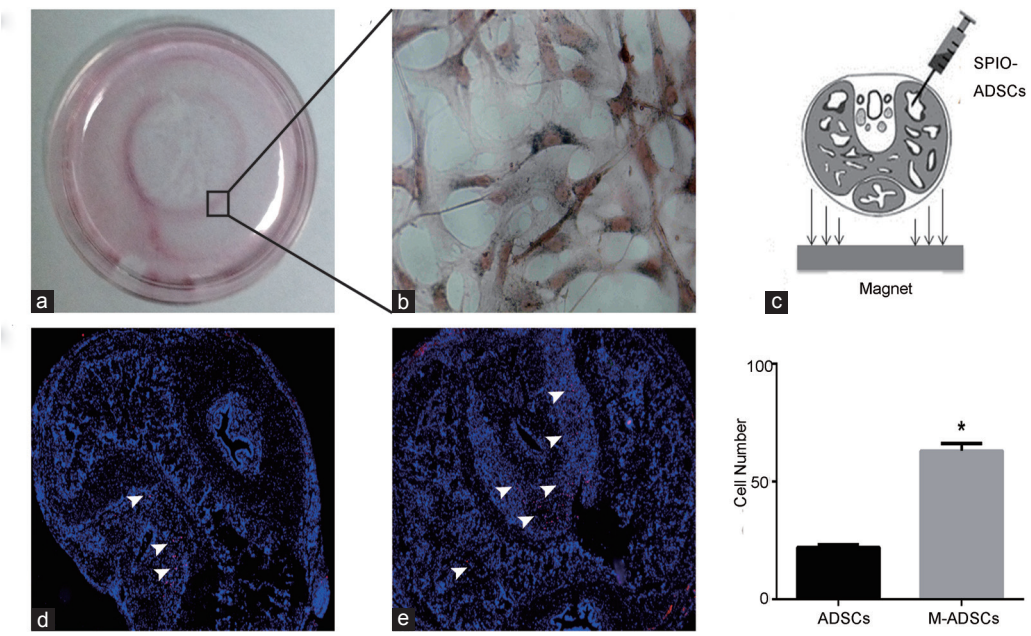

Figure 3: Magnetic field attraction *in vitro* and *in vivo*. (**a**) Clear accumulation of SPION-labeled ADSCs at the edge of the magnet that was placed under the dish at the center for 24 h. The rectangular region is enlarged in (**b**); scale bar = 20 μm. (**c**) Schematic for cell delivery and magnetic forces. Images show EdU+ ADSCs in the corpus cavernosum with (**e**) or without (**d**) magnetic field application. Bar graph presents the numbers of cells homed to the corpus cavernosum. *$P < 0.05$ compared with ADSCs; ADSCs: ADSC-treated group; M-ADSCs: magnetic-targeted group.

injection site for 30 min **(Figure 3c**). To explore whether SPION-labeled ADSCs moved toward the magnetic field applied at the injection site, we labeled ADSCs with EdU. As a result, the number of EdU+ ADSCs was significantly increased in the corpus cavernosum with magnetic field application compared with no application of the magnetic field (**Figure 3d** and **3e**, $P < 0.05$). This result suggested that the SPION-labeled ADSCs responded to exterior magnetic fields both *in vitro* and *in vivo*.

ICP and ICP/MAP

Measurements of erectile function in rats of each experimental group are illustrated in **Figure 4**. Rats in DED group had a significantly lower ICP/MAP ratio than control rats ($P < 0.01$). Moreover, the ICP/MAP ratio in both ADSC-treated groups was significantly higher than that of DED group ($P < 0.01$). In addition, M-ADSC group exhibited more improvement in erectile function than ADSC group ($P < 0.05$).

Fate of transplanted ADSCs in the corpus cavernosum

ADSCs were identified in the corpora cavernosa of diabetic rats at 4 weeks after IC transplantation. EdU+ ADSCs were negative for vWF and α-SMA, indicating that ADSCs did not differentiate into endothelial or smooth muscle cells (**Figure 5**).

Effect of magnetically targeted treatment on the smooth muscle and endothelial contents of the corpus cavernosum

The contents of smooth muscle (indicated by α-SMA) and endothelium (indicated by vWF) in each experimental group are shown in **Figure 6**. At 4 weeks after ADSC transplantation, the smooth muscle and endothelial contents had increased significantly compared with DED group. Moreover, M-ADSC group exhibited more improvement than ADSC group.

VEGF expression in the corpus cavernosum

To explore the paracrine mechanism of transplanted ADSCs, we examined VEGF expression in the corpus cavernosum. The results clearly indicated that VEGF signaling was disrupted in diabetic rats and VEGF expression in the corpus cavernosum was significantly increased in both ADSC-treated groups compared with DED group (**Figure 7**). Moreover, the expression of VEGF in M-ADSC-treated rats was greatly increased compared with that in rats treated with ADSCs only.

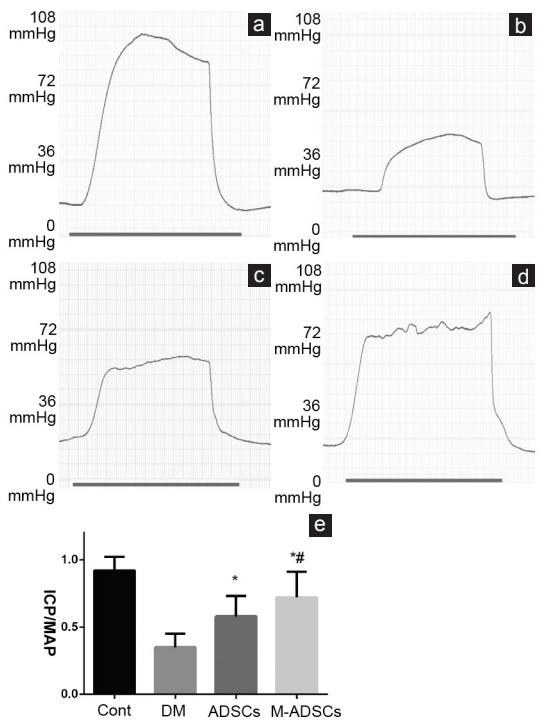

Figure 4: Erectile function evaluation. (**a–d**) Representative recording of ICP in response to electrostimulation of the cavernous nerve. (**e**) Results of erectile function expressed as the ICP/MAP ratio. $^{*}P < 0.05$ compared with DM; $^{\#}P < 0.05$ compared with ADSCs. Cont: normal control group; DM: diabetic group; ADSCs: ADSC-treated group; M-ADSCs: magnetic-targeted group. ICP: intracavernous pressure; MAP: mean arterial pressure.

DISCUSSION

Erection is a neuro-vasculo-tissular phenomenon under hormonal control, which requires the functional integrity of nitrergic nerves, endothelium, and smooth muscles in the penis.[26] However, under experimental hyperglycemic conditions, it has been demonstrated that oxidative stress contributes to neuronal, endothelial, and smooth muscle damage in diabetic animals.[23,27,28] In addition, in diabetic men, the smooth muscle and endothelial density in the corpus cavernosum is reduced significantly.[29] In recent years, it has become clear that cellular therapy can improve erectile function by increasing endothelial and smooth muscle contents in diabetic rats. Thus far, two clinical trials using IC injection of stem cells to treat ED have been carried out. In one study,[30] seven men with type-2 diabetes mellitus and ED were treated by an IC injection of allogeneic umbilical cord blood stem cells. Although only one patient achieved vaginal penetration during an 11-month follow-up, six of the seven patients had their morning erection restored within 3 months. In another study,[31] the authors used autologous bone marrow-derived mononuclear cells (BM-MNCs) to treat 12 men with postradical prostatectomy ED. BM-MNC injection significantly improved most of the sexual scores, and 9 of 12 patients reported successful intercourse with vaginal penetration on medication during the 12-month follow-up. These results suggest that stem cell therapy for ED is a promising approach for future clinical application.

Stem cell migration and homing after transplantation have been a hurdle in the development of regenerative therapies for disorders including ED. Some studies have employed SPIONs, which are typically used as a magnetic resonance imaging contrast agent, to label stem cells and investigate their fate after injection or to guide them to target areas by magnetic field application.[32,33] In the current study, we demonstrated that SPIONs were effectively incorporated into ADSCs without influencing ADSC proliferation or viability *in vitro*. Application of an external magnetic field improved the *in vivo* homing efficiency of SPION-labeled ADSCs to the corpus cavernosum region in a rat model of DED. Further experiments demonstrated that magnetic field-guided SPION-labeled ADSCs contributed to an increase of smooth muscle and endothelial density in the corpus cavernosum and improvement in erectile function compared with treatment with ADSCs alone. Our study provides evidence that magnetic field-guided ADSC therapy is an efficient approach for DED therapy.

In this study, we used a type of commercially available SPION for cell labeling. Traditional SPIONs have some limitations for cell labeling, such as poor labeling efficiency[34] or cytotoxicity.[35] The particle sizes are usually 100–250 nm, which might be too large to be effectively incorporated into cells. However, our *in vitro* and *in vivo* data confirmed that our SPIONs were effectively internalized by ADSCs in the absence of any transfection agent without significantly altering the stem cell properties. In addition, they did not lead to any serious adverse

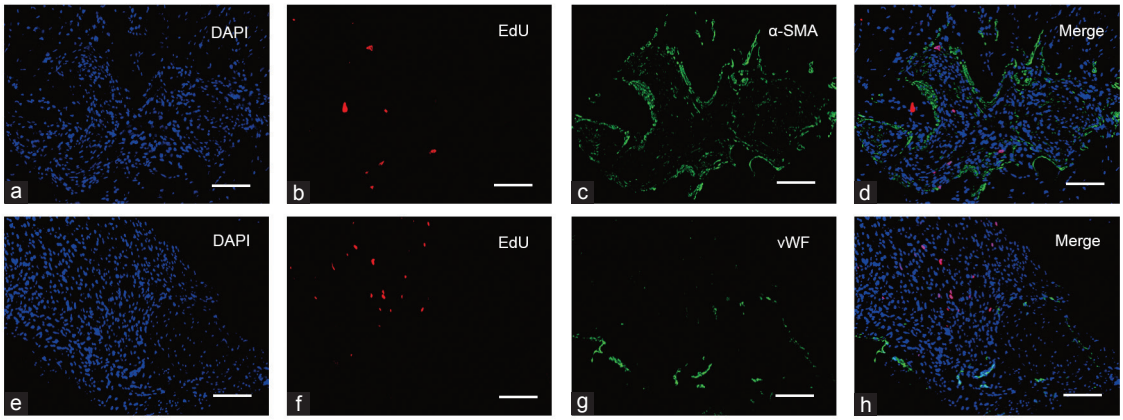

Figure 5: Fate of transplanted ADSCs in the corpus cavernosum. Immunofluorescence analysis of EdU+ ADSCs demonstrated that these cells did not express a smooth muscle cell marker (α-SMA, **a–d**) or endothelial cell marker (vWF, **e–h**) at 4 weeks after ADSC transplantation. Scale bars = 50 μm.

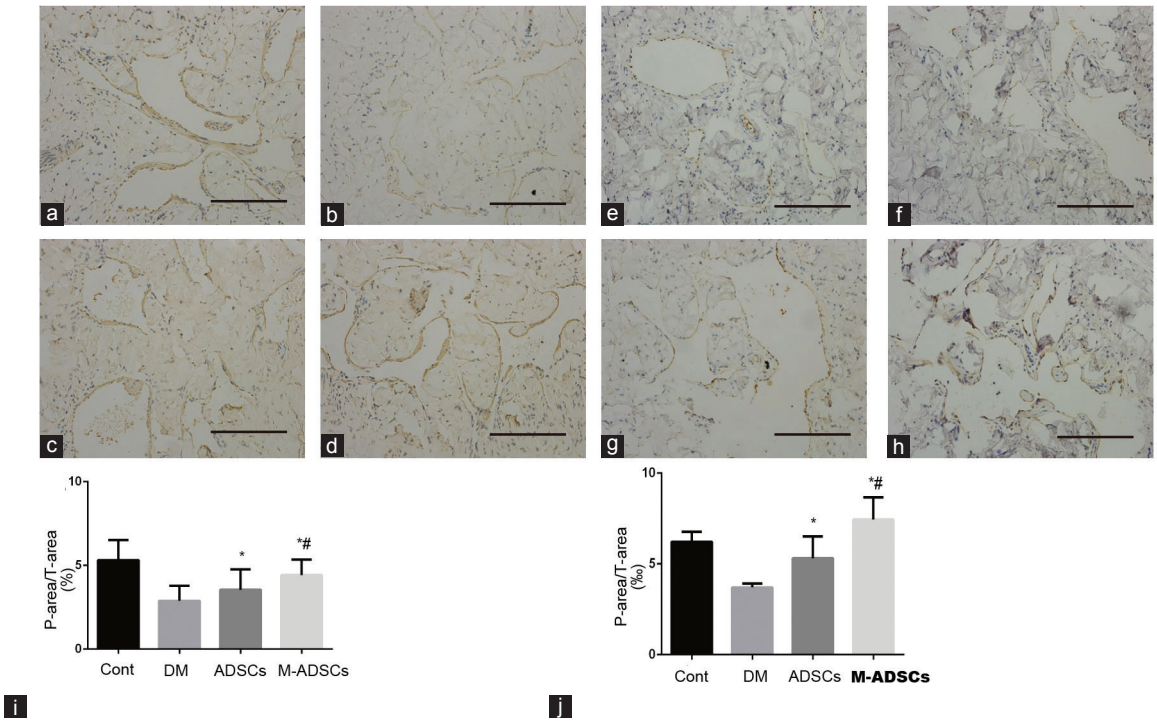

Figure 6: Smooth muscle and endothelial contents in the corpus cavernosum. Immunohistochemical staining of α-SMA in the smooth muscle (**a–d**) and vWF in the endothelium (**e–h**) of each group. Scale bars = 100 μm. Statistical charts represent α-SMA (**i**) and vWF (**j**) densities in each group. $^{*}P < 0.05$ compared with DM; $^{\#}P < 0.05$ compared with ADSCs. Cont: normal control group; DM: diabetic group; ADSCs: ADSC-treated group; M-ADSCs: magnetic-targeted group.

reactions *in vivo*. These properties might be owing to the small size of our SPIONs (10 nm in diameter). It has been shown that recognition of SPIONs by macrophages and systemic clearance depends on the size of the particles, i.e., smaller particles have slower systemic clearance.[36] Notably, immobilization of SPIONs or labeled cells in the blood flow is a complicated process, which requires an external magnetic field with suitable strength. Practically, to resist Brownian and hydrodynamic forces in the blood flow, the field induction should be ≥1 T, which can be easily achieved using powerful permanent magnets based on neodymium-iron alloys.[37]

Our immunofluorescence results revealed that ADSCs survived in the corpus cavernosum for at least 4 weeks, and they did not express smooth muscle or endothelial cell markers. These data showed that transplanted ADSCs might exert paracrine effects to improve erectile function in STZ-induced diabetic rats. It has been increasingly observed that transplanted MSCs might exert their therapeutic effects through secreting a variety of autocrine/paracrine factors, called the secretome,[38] or exosomes enriched with distinctive miRNA and tRNA species.[39] However, in our study, we only assessed the expression of VEGF in the corpus cavernosum. Unexpectedly, we found that local delivery of ADSCs significantly increased VEGF expression in the corpus cavernosum. Moreover, M-ADSC group appeared to exhibit higher VEGF expression. The molecular mechanisms of the therapeutic effects of ADSCs on ED should be investigated further.

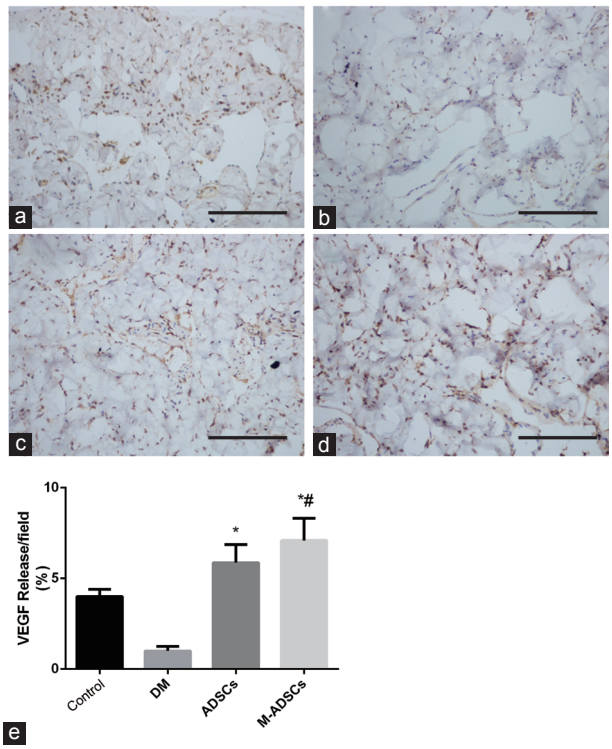

Figure 7: VEGF expression in the corpus cavernosum. Immunohistochemical staining demonstrated dark brown VEGF-positive areas in each group (**a–d**). (**e**) Statistical charts represent the VEGF density in each group. Scale bars = 100 μm. $^{*}P < 0.05$ compared with DM; $^{\#}P < 0.05$ compared with ADSCs. Cont: normal control group; DM: diabetic group; ADSCs: ADSC-treated group; M-ADSCs: magnetic-targeted group.

Our study has some limitations. First, we did not investigate exocytosis or cellular transport of SPIONs. Only one study has shown that human umbilical vein endothelial cells uptake mesoporous silica nanoparticles effectively after 13 min of incubation while all mesoporous silica nanoparticles migrate from the interior of the cells to the periphery at 37 min after incubation.[40] Interestingly, it has been demonstrated that cells exchange particles with each other through a series of cross-cell experiments. Moreover, iron oxide nanoparticle-mediated development of cellular gap junction crosstalk among cells improves the therapeutic efficacy of MSCs in myocardial infarction.[41] The molecular mechanisms of the interaction of SPIONs with stem cell biology should be investigated further. Second, we used 30 min as the magnetic attraction time, which might not be the most suitable duration. However, based on our results, brief magnetic attraction successfully facilitated ADSC homing to the corpus cavernosum region. Although this phenomenon may be a "butterfly effect" as reported by Cheng *et al.*[33] and Li *et al.*[24] who placed magnets at the target areas for 10 and 120 min, respectively, magnetic targeting improved short-term cell retention, which in turn boosted long-term engraftment.

In this study, IC transplantation of ADSCs restored the impairment of erectile function in diabetic rats. SPIONs were effectively incorporated into ADSCs without altering the stem cell properties. External magnetic field application improved the efficiency of SPION-labeled ADSC homing to the corpus cavernosum region and contributed to the improvement in erectile function compared with ADSC treatment alone. Through further elucidation of the potential mechanisms of functional and structural recovery, it appeared that paracrine effects of ADSCs played the major role in these recoveries. Our study provides evidence that magnetic field-guided ADSC therapy is an efficient approach for DED treatment.

AUTHOR CONTRIBUTIONS

LLZ, ZZ, and HSJ performed the experiment; LLZ, YC, and YTD participated in the design of the study and performed the statistical analyses. LLZ and YTD wrote the manuscript. All authors read and approved the final manuscript.

COMPETING FINANCIAL INTERESTS

The authors have declared that there are no competing financial interests.

ACKNOWLEDGMENTS

The present study was supported by the National Natural Scientific Foundation of China Grants (No. 81170563 and 81270694).

REFERENCES

1 Malavige LS, Levy JC. Erectile dysfunction in diabetes mellitus. *J Sex Med* 2009; 6: 1232–47.
2 Richardson D, Vinik A. Etiology and treatment of erectile failure in diabetes mellitus. *Curr Diab Rep* 2002; 2: 501–9.
3 Moore CR, Wang R. Pathophysiology and treatment of diabetic erectile dysfunction. *Asian J Androl* 2006; 8: 675–84.
4 Gur S, Peak TC, Kadowitz PJ, Sikka SC, Hellstrom WJ. Review of erectile dysfunction in diabetic animal models. *Curr Diabetes Rev* 2014; 10: 61–73.
5 Vickers MA, Satyanarayana R. Phosphodiesterase type 5 inhibitors for the treatment of erectile dysfunction in patients with diabetes mellitus. *Int J Impot Res* 2002; 14: 466–71.
6 Lin CS, Xin ZC, Wang Z, Deng C, Huang YC, *et al.* Stem cell therapy for erectile dysfunction: a critical review. *Stem Cells Dev* 2012; 21: 343–51.
7 Liu G, Sun X, Bian J, Wu R, Guan X, *et al.* Correction of diabetic erectile dysfunction with adipose derived stem cells modified with the vascular endothelial growth factor gene in a rodent diabetic model. *PLoS One* 2013; 8: e72790.
8 Ouyang B, Sun X, Han D, Chen S, Yao B, *et al.* Human urine-derived stem cells alone or genetically-modified with FGF2 Improve type 2 diabetic erectile dysfunction in a rat model. *PLoS One* 2014; 9: e92825.
9 Sun C, Lin H, Yu W, Li X, Chen Y, *et al.* Neurotrophic effect of bone marrow mesenchymal stem cells for erectile dysfunction in diabetic rats. *Int J Androl* 2012; 35: 601–7.
10 Qiu X, Lin H, Wang Y, Yu W, Chen Y, *et al.* Intracavernous transplantation of bone marrow-derived mesenchymal stem cells restores erectile function of streptozocin-induced diabetic rats. *J Sex Med* 2011; 8: 427–36.
11 Huang SJ, Fu RH, Shyu WC, Liu SP, Jong GP, *et al.* Adipose-derived stem cells: isolation, characterization, and differentiation potential. *Cell Transplant* 2013; 22: 701–9.
12 Garcia MM, Fandel TM, Lin G, Shindel AW, Banie L, *et al.* Treatment of erectile dysfunction in the obese type 2 diabetic ZDF rat with adipose tissue-derived stem cells. *J Sex Med* 2010; 7: 89–98.
13 Xu Y, Guan R, Lei H, Li H, Wang L, *et al.* Therapeutic potential of adipose-derived stem cells-based micro-tissues in a rat model of postprostatectomy erectile dysfunction. *J Sex Med* 2014; 11: 2439–48.
14 Neri M, Maderna C, Cavazzin C, Deidda-Vigoriti V, Politi LS, *et al.* Efficient *in vitro* labeling of human neural precursor cells with superparamagnetic iron oxide particles: relevance for *in vivo* cell tracking. *Stem Cells* 2008; 26: 505–16.
15 Wang Y, Xu F, Zhang C, Lei D, Tang Y, *et al.* High MR sensitive fluorescent magnetite nanocluster for stem cell tracking in ischemic mouse brain. *Nanomedicine* 2011; 7: 1009–19.
16 Song M, Kim YJ, Kim YH, Roh J, Kim SU, *et al.* Using a neodymium magnet to target delivery of ferumoxide-labeled human neural stem cells in a rat model of focal cerebral ischemia. *Hum Gene Ther* 2010; 21: 603–10.
17 Riegler J, Liew A, Hynes SO, Ortega D, O'Brien T, *et al.* Superparamagnetic iron oxide nanoparticle targeting of MSCs in vascular injury. *Biomaterials* 2013; 34: 1987–94.
18 Schafer R, Bantleon R, Kehlbach R, Siegel G, Wiskirchen J, *et al.* Functional investigations on human mesenchymal stem cells exposed to magnetic fields and labeled with clinically approved iron nanoparticles. *BMC Cell Biol* 2010; 11: 22.
19 Chen CH, Lin YS, Fu YC, Wang CK, Wu SC, *et al.* Electromagnetic fields enhance chondrogenesis of human adipose-derived stem cells in a chondrogenic microenvironment *in vitro*. *J Appl Physiol (1985)* 2013; 114: 647–55.
20 Saha S, Yang XB, Tanner S, Curran S, Wood D, *et al.* The effects of iron oxide incorporation on the chondrogenic potential of three human cell types. *J Tissue Eng Regen Med* 2013; 7: 461–9.

21 Qi Y, Feng G, Huang Z, Yan W. The application of super paramagnetic iron oxide-labeled mesenchymal stem cells in cell-based therapy. *Mol Biol Rep* 2013; 40: 2733–40.
22 Yu W, Wan Z, Qiu XF, Chen Y, Dai YT. Resveratrol, an activator of SIRT1, restores erectile function in streptozotocin-induced diabetic rats. *Asian J Androl* 2013; 15: 646–51.
23 Qiu X, Villalta J, Ferretti L, Fandel TM, Albersen M, *et al*. Effects of intravenous injection of adipose-derived stem cells in a rat model of radiation therapy-induced erectile dysfunction. *J Sex Med* 2012; 9: 1834–41.
24 Li Q, Tang G, Xue S, He X, Miao P, *et al*. Silica-coated superparamagnetic iron oxide nanoparticles targeting of EPCs in ischemic brain injury. *Biomaterials* 2013; 34: 4982–92.
25 Albersen M, Fandel TM, Lin G, Wang G, Banie L, *et al*. Injections of adipose tissue-derived stem cells and stem cell lysate improve recovery of erectile function in a rat model of cavernous nerve injury. *J Sex Med* 2010; 7: 3331–40.
26 Gratzke C, Angulo J, Chitaley K, Dai YT, Kim NN, *et al*. Anatomy, physiology, and pathophysiology of erectile dysfunction. *J Sex Med* 2010; 7: 445–75.
27 Vlassara H, Fuh H, Makita Z, Krungkrai S, Cerami A, *et al*. Exogenous advanced glycosylation end products induce complex vascular dysfunction in normal animals: a model for diabetic and aging complications. *Proc Natl Acad Sci U S A* 1992; 89: 12043–7.
28 Jeremy JY, Jones RA, Koupparis AJ, Hotston M, Persad R, *et al*. Reactive oxygen species and erectile dysfunction: possible role of NADPH oxidase. *Int J Impot Res* 2007; 19: 265–80.
29 Yaman O, Yilmaz E, Bozlu M, Anafarta K. Alterations of intracorporeal structures in patients with erectile dysfunction. *Urol Int* 2003; 71: 87–90.
30 Bahk JY, Jung JH, Han H, Min SK, Lee YS. Treatment of diabetic impotence with umbilical cord blood stem cell intracavernosal transplant: preliminary report of 7 cases. *Exp Clin Transplant* 2010; 8: 150–60.
31 Yiou R, Hamidou L, Birebent B, Bitari D, Lecorvoisier P, *et al*. Safety of intracavernous bone marrow-mononuclear cells for postradical prostatectomy erectile dysfunction: an open dose-escalation pilot study. *Eur Urol* 2015. [Epub ahead of print].
32 Song YS, Ku JH, Song ES, Kim JH, Jeon JS, *et al*. Magnetic resonance evaluation of human mesenchymal stem cells in corpus cavernosa of rats and rabbits. *Asian J Androl* 2007; 9: 361–7.
33 Cheng K, Li TS, Malliaras K, Davis DR, Zhang Y, *et al*. Magnetic targeting enhances engraftment and functional benefit of iron-labeled cardiosphere-derived cells in myocardial infarction. *Circ Res* 2010; 106: 1570–81.
34 Arbab AS, Yocum GT, Wilson LB, Parwana A, Jordan EK, *et al*. Comparison of transfection agents in forming complexes with ferumoxides, cell labeling efficiency, and cellular viability. *Mol Imaging* 2004; 3: 24–32.
35 Chen Z, Yin JJ, Zhou YT, Zhang Y, Song L, *et al*. Dual enzyme-like activities of iron oxide nanoparticles and their implication for diminishing cytotoxicity. *ACS Nano* 2012; 6: 4001–12.
36 Fang C, Shi B, Pei YY, Hong MH, Wu J, *et al*. *In vivo* tumor targeting of tumor necrosis factor-alpha-loaded stealth nanoparticles: effect of MePEG molecular weight and particle size. *Eur J Pharm Sci* 2006; 27: 27–36.
37 Reddy LH, Arias JL, Nicolas J, Couvreur P. Magnetic nanoparticles: design and characterization, toxicity and biocompatibility, pharmaceutical and biomedical applications. *Chem Rev* 2012; 112: 5818–78.
38 Kupcova Skalnikova H. Proteomic techniques for characterisation of mesenchymal stem cell secretome. *Biochimie* 2013; 95: 2196–211.
39 Baglio SR, Rooijers K, Koppers-Lalic D, Verweij FJ, Perez Lanzon M, *et al*. Human bone marrow- and adipose-mesenchymal stem cells secrete exosomes enriched in distinctive miRNA and tRNA species. *Stem Cell Res Ther* 2015; 6: 127.
40 Slowing II, Vivero-Escoto JL, Zhao Y, Kandel K, Peeraphatdit C, *et al*. Exocytosis of mesoporous silica nanoparticles from mammalian cells: from asymmetric cell-to-cell transfer to protein harvesting. *Small* 2011; 7: 1526–32.
41 Han J, Kim B, Shin JY, Ryu S, Noh M, *et al*. Iron oxide nanoparticle-mediated development of cellular gap junction crosstalk to improve mesenchymal stem cells' therapeutic efficacy for myocardial infarction. *ACS Nano* 2015; 9: 2805–19.

This is an open access article distributed under the terms of the Creative Commons Attribution-NonCommercial-ShareAlike 3.0 License, which allows others to remix, tweak, and build upon the work non-commercially, as long as the author is credited and the new creations are licensed under the identical terms.

©The Author(s)(2017)